

Nonlinear sensor fault diagnosis in wireless sensor networks using structural response data

Kosmas Dragos, Kay Smarsly
Chair of Computing in Civil Engineering
Bauhaus University Weimar, Germany

Katrin Jahr
Chair of Computational Modelling and Simulation
Technical University Munich, Germany
katrin.jahr@tum.de

Abstract. This paper introduces a novel approach towards sensor fault diagnosis in wireless structural health monitoring systems. As compared to traditional fault diagnosis approaches, a number of innovations are reported in this paper. First, by embedding fault models and algorithms directly into wireless sensor nodes, sensor faults can be self-detected by the nodes in a distributed-cooperative fashion. Second, no redundant sensor installations are required for fault diagnosis, because the wireless sensor nodes exploit the redundant information of correlated sensors already installed in the monitored structure (“analytical redundancy”). Third, instead of using raw time series of sensor data for analytical redundancy, the sensor data is first transformed from the time domain into the frequency domain on-board the sensor nodes, entailing significantly reduced data traffic. Fourth, nonlinearities in the data sets (e.g. due to measurement factors) are handled by implementing the analytical redundancy approach in terms of feedforward backpropagation neural networks embedded into the wireless sensor nodes. Fifth, due to the adaptation abilities of the embedded neural networks, sensor fault diagnosis remains efficient and accurate even if the monitored structure is subject to structural changes (or damage) as reflected in the sensor data. Sixth, no a priori knowledge about the structure or about the sensor instrumentation is required because the neural networks, representing a purely data-driven approach, take previously collected sensor data as the sole basis for fault diagnosis. This paper presents the fault diagnosis methodology, followed by the implementation into a fault-tolerant wireless structural health monitoring system prototype. Validation experiments on a laboratory test structure demonstrate the efficiency and accuracy of the proposed approach.

1. Introduction

Structural health monitoring (SHM) is increasingly employed for assessing the condition of civil engineering structures. In the field of SHM, wireless sensor networks have been gaining growing popularity over conventional cable-based systems, due to the advantages of easy and cost-effective installation of wireless sensor nodes. Moreover, the on-board processing power of wireless sensor nodes has been utilized in many research approaches for embedding algorithms that execute various monitoring tasks (Dragos and Smarsly, 2015).

Wireless SHM systems, operating in harsh environments over long periods of time, are vulnerable to sensor faults and sensor miscalibrations. Sensor faults affect the reliable and accurate operation of SHM systems, resulting in errors (manifestations of sensor faults), which lead to failures detectable in sensor outputs. The detection and isolation of sensor faults, hereinafter for simplification referred to as “fault diagnosis”, has been a topic of ongoing investigation since about 40 years (Willsky, 1976). Fault diagnosis approaches usually rely on residuals between predicted and actual sensor outputs, typically structural response data (Smarsly and Petryna, 2014). The comparison between predicted and actual sensor outputs is performed either by installing redundant sensors (“physical redundancy”) or

by using the redundant information obtained by existing sensors (“analytical redundancy”). In both cases, the calculation of predicted outputs is based on the inherent correlations in the structural response data obtained from different locations of the structure (Kraemer and Fritzen, 2007). According to the available information on the properties of the structure, the correlations in the structural response data is derived either from physics-based models (e.g. finite element models) or from data-driven models (e.g. artificial neural networks).

Sensor fault detection based on artificial neural networks (ANNs) has been a topic of extensive research. For instance, the detection of process failures (e.g. sensor faults) using various neural network topologies has been proposed by Venkatasubramanian et al. (1990). Obst (2009) has introduced a sensor fault detection schema employing a distributed recurrent neural network. In their fault detection approach, Basirat and Khan (2009) have presented an ANN-based method for distinguishing faulty sensor data from non-faulty sensor data. The use of analytical redundancy in the correlations between sensor outputs for detecting sensor faults in wireless SHM systems has been proposed by Smarsly and Law (2014) by mapping both the characteristics of the structure and the correlations among the sensors.

In the approaches reported so far, fault diagnosis, performed either in a centralized or decentralized manner, entails a non-negligible wireless communication load due to the utilization of raw sensor data. This paper presents a novel approach towards fault diagnosis in wireless structural health monitoring systems based on processed structural response data, enabling wireless sensor nodes to self-diagnose sensor faults and miscalibrations. The diagnosis of sensor faults is performed by exploiting correlations among Fourier amplitudes of acceleration response data from different sensors, at peaks of the corresponding frequency spectra indicative of structural modes of vibration. More specifically, for a given structural condition, predictions of Fourier amplitudes for each sensor node are obtained using the Fourier amplitudes of other sensor nodes as input data. Residuals between the predicted and the actual Fourier amplitudes, obtained from the transformation of newly collected acceleration response data, exceeding a predefined threshold are indicative of sensor faults. While in theory Fourier amplitudes of acceleration response data from different locations of the structure are linearly connected, in practice, due to several factors, deviations from linearity are observed. The fault diagnosis approach presented in this study is nonlinear and entirely data-driven, requiring no knowledge on the characteristics of the structure. To this end, for the derivation of predicted Fourier amplitudes, ANNs are employed. Laboratory experiments are conducted for validating the proposed approach, demonstrating the efficiency of the approach in detecting sensor faults.

First, the background of the fault diagnosis approach is illuminated, and the implementation into a wireless SHM system is described. Second, the validation tests of the proposed approach are presented. Finally, results of the validation tests as well as potential future research directions are discussed.

2. Mathematical background

In this section, the mathematical background of the proposed methodology is elucidated, followed by the design principles developed for implementation of the methodology into a fault-tolerant wireless SHM system prototype.

2.1 Spectral density

In signal processing, spectral density represents the amount of energy carried by a signal. Considering a continuous function $f(t)$ of time, the spectral density S is defined as

$$S = \int_{-\infty}^{+\infty} |f(t)|^2 dt \quad (1)$$

It can be proven that spectral density is directly related to the autocorrelation of a signal. Indeed, according to Parseval's theorem, if the Fourier transform of the signal (the transformation of the signal into the frequency domain) exists, the spectral density and the Fourier transform are related as shown in Eq. 2.

$$\int_{-\infty}^{+\infty} |f(t)|^2 dt = \int_{-\infty}^{+\infty} |F(\omega)|^2 d\omega \quad S(\omega) = \lim_{T \rightarrow \infty} \mathbf{E} |F(\omega)|^2 \quad (2)$$

In Eq. 2, \mathbf{E} denotes the expected value and ω is the eigenfrequency. For a time lag τ , Eq. 2 is transformed as follows:

$$S(\omega) = \lim_{T \rightarrow \infty} \mathbf{E} \left[\int_{-T}^{+T} f(t) e^{i\omega t} \overline{f(t+\tau)} e^{-i\omega(t+\tau)} dt \right] = \int_{-\infty}^{+\infty} R(\tau) e^{-i\omega\tau} d\tau = R(\omega) \quad (3)$$

where $R(\omega)$ is the autocorrelation function of signal $f(t)$ at time lag τ . The overbar denotes complex conjugate. If two different signals are used in Eq. 3, the cross spectral density is obtained, which is essentially the cross correlation function of the two signals. If the signals in Eq. 1, Eq. 2, and Eq. 3 represent acceleration response data sets, the correlations among the response data sets can be extended to the transformed response data sets, i.e. to the corresponding frequency spectra. It has been also proven that these correlations in the frequency domain are stronger at the peaks of the frequency spectrum indicative of structural modes of vibration – a feature used for modal identification (Brincker et al., 2000).

2.2 Fault diagnosis using the correlations among Fourier amplitudes

As shown in Figure 1, four fault types can be distinguished: bias, drift, complete failure, and precision degradation (Qin and Li, 1999). Bias is the deviation by a constant value between sensor output and actual structural output. Drift is the incrementing deviation between sensor outputs and actual structural outputs. In case of complete failure, the sensor outputs remain constant regardless of changes in the actual structural outputs, while in precision degradation the sensor outputs are contaminated with a white noise function.

All fault types affect the amplitudes of the frequency spectrum; however, it should be noted that the effect of each fault on the Fourier amplitudes, at the peaks used for fault diagnosis, varies. For example, sensor faults usually introduce unwanted frequency components into the frequency spectrum, but the contamination of the frequency spectrum is not uniform at all frequencies. Hence, if the effects of a sensor fault on the amplitudes at potential modal peaks used for fault diagnosis are small, the respective fault might be undetectable.

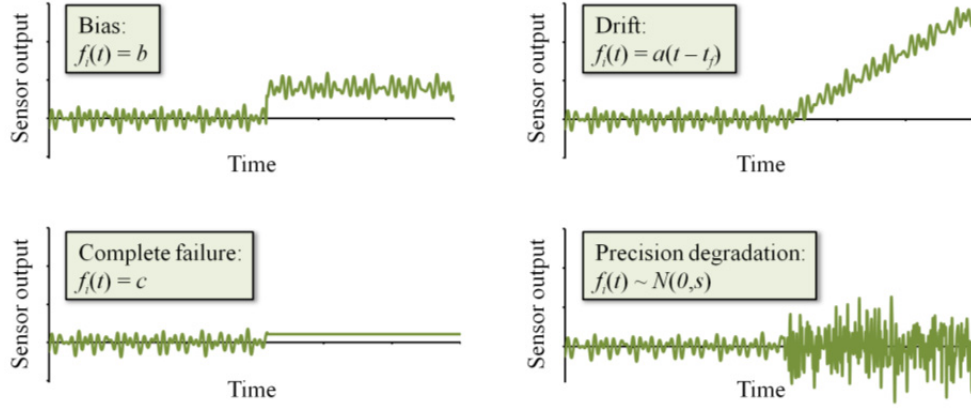


Figure 1: Categories of sensor faults in SHM systems

From structural dynamics, it is proven that the relationship among the Fourier amplitudes of acceleration responses from different locations of the structure at modal peaks is linear. However, in experimental dynamics, due to measurement factors, a deviation from linearity among the Fourier amplitudes of acceleration response data from different sensors is observed. For example, if a mode is not well excited, the Fourier amplitudes at the respective peak correspond to an “operating deflection shape”, rather than the exact mode shape, and the linear relationship among the amplitudes does not hold. Furthermore, “round-off” errors (also referred to as “quantization errors” or “quantization noise”), following the analog-to-digital conversion, also introduce nonlinearities in the relationships among Fourier amplitudes. Finally, similar effects on frequency spectra are observed due to the presence of ambient noise. Figure 2 illustrates the nonlinearities introduced into the relationships among Fourier amplitudes, due to the aforementioned factors, for an arbitrary structure subjected to N different excitations.

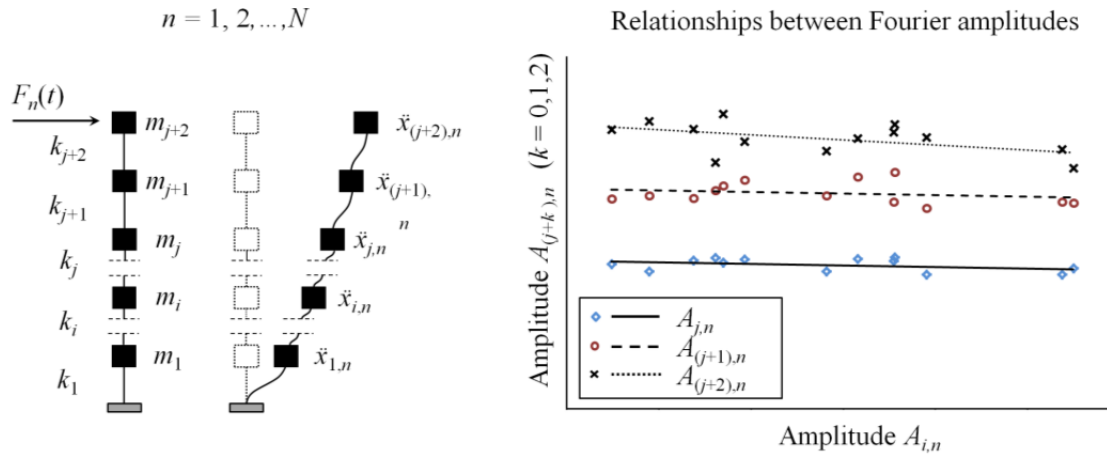


Figure 2: Nonlinear relationships between Fourier amplitudes of acceleration response data from different locations of a structure

3. Implementation of the fault diagnosis approach into a wireless SHM system

A wireless SHM system prototype is employed to implement the proposed fault diagnosis approach. In this section, the components of the SHM system are described and the embedded software is presented, with particular focus on the fault diagnosis tasks.

3.1 Components of the wireless structural health monitoring system

The SHM system comprises wireless sensor nodes, a gateway node (denoted as “base station”), and a host computer communicating with the sensor nodes via the base station. As illustrated in Figure 3, the monitoring tasks executed by the SHM system are: 1) data acquisition, 2) data processing, 3) fault diagnosis, 4) data transmission, 5) data storage, and 6) data analysis. Data acquisition is essentially the collection of acceleration response data, while data processing involves the transformation of the collected acceleration response data into the frequency domain, using the Cooley-Tukey FFT algorithm (Cooley and Tukey, 1968). Data processing is completed by the detection of the highest peak of the frequency spectrum, typically corresponding to the fundamental (first) mode of vibration. Subsequently, fault diagnosis is conducted through cooperative analysis among the sensor nodes. Tasks 1, 2, and 3 are executed on-board the sensor nodes. The processed data is wirelessly communicated to the host computer through the base station (task 4), where the data is stored and analyzed (tasks 5 and 6).

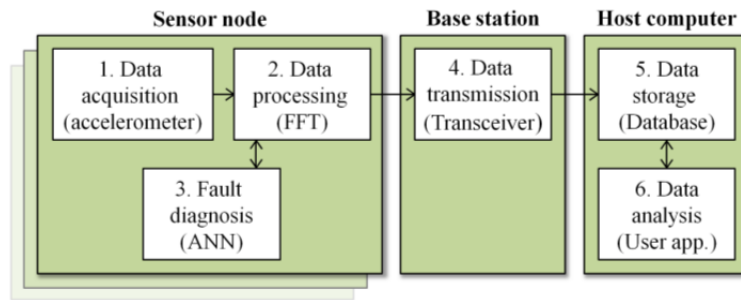


Figure 3: Monitoring tasks supported by the fault-tolerant wireless SHM system

The proposed fault diagnosis approach follows the concept of analytical redundancy, implemented in terms of ANNs embedded into the wireless sensor nodes. The embedded ANNs consist of several neurons structured in three layers. Considering an arbitrary sensor node j of the SHM system, the topology of the embedded ANN is given in Figure 4. The actual k amplitudes received from $1 \dots k$ neighboring sensor nodes are fed to the input layer. Because of the nonlinearity in the relationship among the Fourier amplitudes of different sensor nodes, the output of the ANN (i.e. the predicted Fourier amplitude) cannot be directly obtained from the input data. Therefore, according to the ANN theory, a hidden layer of m neurons is added to accommodate the nonlinear relationship between the input layer and the output layer. In the output layer, the predicted amplitude of sensor node j is obtained. The synapses, i.e. the neuron connections, define the data exchange rate between the neurons.

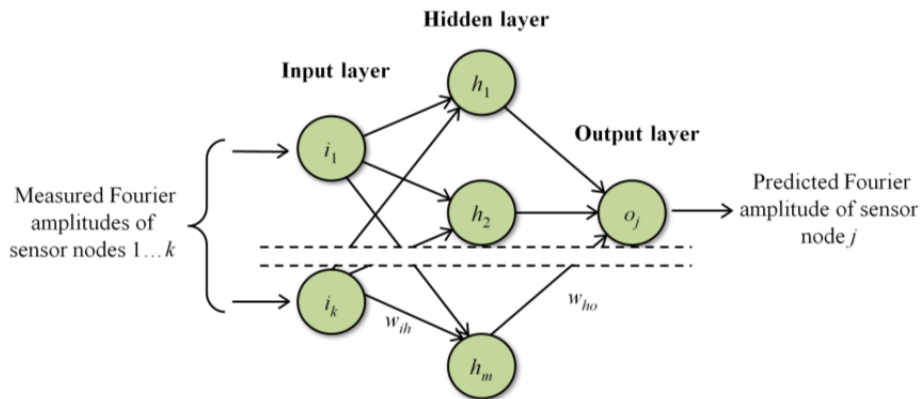


Figure 4: Artificial neural network embedded into sensor node j

The ANNs are trained by adjusting the weights of the synapses until the desired predicted Fourier amplitude of sensor node j is obtained. In a final step, the ANN properties, i.e. the topology (the number of neurons per layer) and the behavior of the neurons (the functions connecting the output of each neuron to the input of the next neuron), are defined.

3.2 Architecture of the embedded software

For operating the SHM system, embedded software is written in Java programming language. In particular, two packages have been developed, one for managing the tasks of the sensor nodes (package “sensornode”) and one for handling the tasks of the host computer (package “server”).

In the `sensornode` package, Java classes that perform the three sensor node tasks, as described in Figure 3, as well as the wireless communication to the base station, are included. The classes `AccelerationSampler` and `Sample` are responsible for data acquisition; the class `FFT` handles data processing, while the class `Communication` is used for establishing wireless communication links to the base station. Fault diagnosis is performed by the classes `NetworkTraining` and `MainNode`. For the implementation of ANN tasks, the external ANN library SNIPE is used (Kriesel, 2010). An extract of the `sensornode` package is provided in Figure 5.

The package `server` contains Java classes to perform the server tasks. For example, the class `MainBase` handles the communication between the base station and the sensor nodes. The `Sample` class manages the information received by the sensor nodes, converting it to the desired form to be stored into the database. Finally, the class `DatabaseHandler` is used to connect to a MySQL database, where the information packaged by the `Sample` class (eigenfrequencies and amplitudes calculated by the sensor nodes, sensor IDs, and fault diagnosis assessment) is stored.

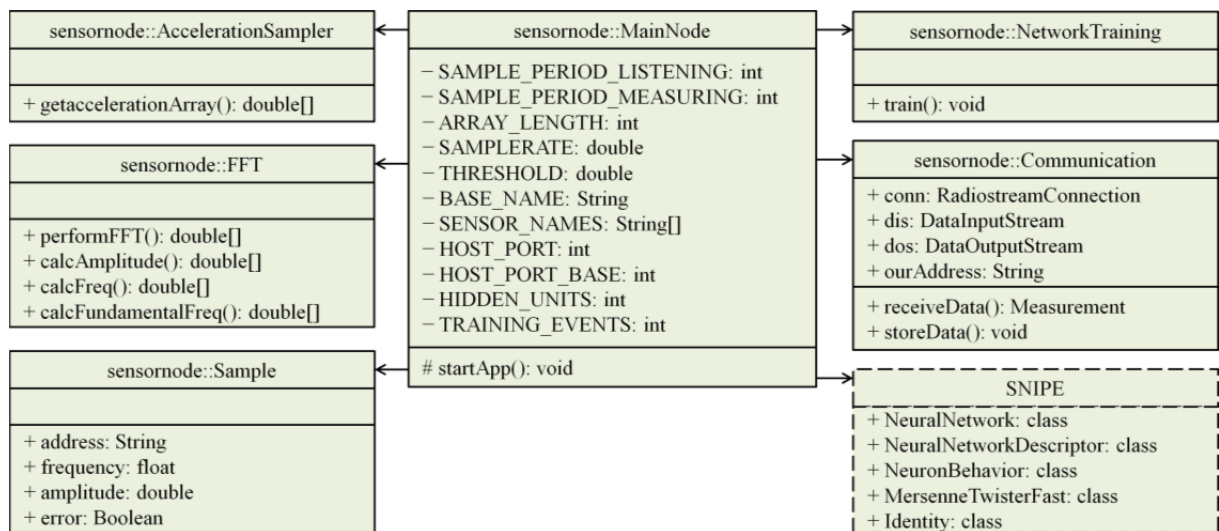


Figure 5: Extract of the “sensornode” package

4. Validation tests

Validation tests for the proposed fault diagnosis approach are conducted for demonstrating the ability of the approach to detect faults at a given structural condition. In this section, the validation tests are described, including the definition of the (case-specific) ANN properties and the application of the approach on a laboratory test structure.

4.1 Laboratory test setup

For the validation tests conducted in this study, Oracle Sun SPOT sensor nodes are employed (Oracle Corp., 2010). A sensor node includes an integrated digital output MEMS accelerometer, type MMA7455L, with a measurement range from $\pm 2g$ to $\pm 8g$. The test structure employed for the validation tests is a 4-story steel frame structure. Each story slab is a steel sheet of $250\text{ mm} \times 500\text{ mm} \times 0.8\text{ mm}$ (length \times width \times thickness) dimensions, resting on four M5 steel threaded rods representing the columns of the structure. The frame structure is fixed at the column bases into a solid block (Figure 6).

In this study, two common fault types are exemplarily simulated: bias and precision degradation. Bias faults often occur when there is partial loss of connectivity of the sensor to the structure. For simulating the bias, sensor node *B* is rotated by 45° with respect to the initial position, as shown in Figure 6b. The ANN properties are first defined and the selected ANNs are trained by collecting acceleration response data from the unfaulty state (Figure 6a). Fault diagnosis is performed by using acceleration response data from the two faulty states: for the bias fault, acceleration response data from the state depicted in Figure 6b is used, while for precision degradation, the collected acceleration response data from the unfaulty state is contaminated by excessive variance white noise.



Figure 6: (a) Laboratory test setup and (b) simulated sensor fault

4.2 Definition of artificial neural network properties

The definition of the ANN properties depends on the structural properties (i.e. it is case-specific) and is based on prediction accuracy, i.e. the deviations between the predicted Fourier amplitudes (F_{pred}) and the actual Fourier amplitudes (F_{act}) (Eq. 4), and on performance, i.e. the time used to derive the output. Since the training of the ANNs also requires the adjustment of the weights until the desired output is obtained, the definition of the ANN properties essentially coincides with the ANN training.

$$\varepsilon_{RMS} = \sqrt{\frac{\sum_{i=1}^N F_{pred_i}(\omega_1)^2 - F_{act_i}(\omega_1)^2}{N}} \quad (4)$$

In Eq. 4, ε_{RMS} is the root mean square error between F_{pred} and F_{act} , at iteration i of the ANN training, ω_1 is the fundamental eigenfrequency, which characterizes the structural condition, and N is the number of samples, i.e. sets of input and output values. In this study, the data set used for selecting the ANN properties contains 100 Fourier amplitudes at the fundamental eigenfrequency derived on-board the sensor nodes from collected acceleration response data under free vibration. Each data set is divided into a training set for adjusting the neuron weights, a validation set for monitoring the training process, and a test set for confirming the predictive power of the ANN. Several ANN topologies and neuron behaviors are tested, the results of which are summarized in Table 1. Based on the results shown in Table 1, an ANN with 3-2-1 topology and interlayer backpropagation neuron behaviour is selected, considering a reasonable trade-off between the selection criteria, i.e. low prediction error as well as low computation time.

Table 1: Definition of ANN properties based on prediction accuracy and performance

Neuron behavior	Topology	Neurons/node	Computation time (s)	ε_{RMS} (-)
Interlayer, backpropagation	3-1	4	6.6	0.149
	3-2-1	6	13.0	0.096
	3-3-1	7	17.2	0.144
	3-5-1	9	25.0	0.081
	3-7-1	11	32.2	0.063
	3-2-2-1	8	21.0	0.092
	3-5-5-1	14	46.6	0.137
Interlayer and supralayer, backpropagation	3-3-1	7	15.2	0.147
	3-5-1	9	22.6	0.132
	3-2-2-1	8	19.4	0.137
Interlayer, resilient backpropagation	3-3-1	7	113.0	0.153
	3-5-1	9	172.4	0.143
	3-2-2-1	8	120.6	0.208

4.3 Operation of the fault-tolerant SHM system

Using the defined ANN properties, the operation of the SHM system is performed at the two faulty states. First, the bias fault type is simulated on sensor node B , as shown in Figure 6b. The test structure is excited by imposing a deflection at the top story and by removing the deflection force. Acceleration response data is collected under free vibration and, on-board the sensor nodes, transformed into the frequency domain. The embedded peak detection algorithms on the nodes pick the amplitudes that corresponds to the fundamental eigenfrequency, in an attempt to verify that the structural condition remains unaltered with respect to the ANN training stage. Subsequently, 30 sets of acceleration response data are collected and the corresponding Fourier amplitudes are calculated by all sensor nodes. Then, the amplitudes from sensor nodes A , C , and D are fed into the ANN of sensor node B as input

data, and the predicted Fourier amplitude of the sensor node is derived. Finally, the root mean square error ($\epsilon_{RMS,30}$) of the residual between the predicted Fourier amplitude and the actual Fourier amplitude of sensor node B is calculated for the Fourier amplitudes of the 30 acceleration response data sets. For precision degradation, a similar testing procedure is followed. However, the test is conducted using the setup shown in Figure 6a, because the fault is injected into sensor node B by adding random values to the collected acceleration response data.

Drawing from the benchmark ϵ_{RMS} values of Table 1 for non-faulty operation, the threshold for fault diagnosis is set to $\tau = 0.150$. The results of the operation of the SHM system are summarized in Table 2.

Table 2: Fault diagnosis of simulated sensor faults, indicated by root mean square error.

Root mean square error (30 data sets)	Non-faulty operation	Faulty operation	
		Bias	Precision degradation
$\epsilon_{RMS,30}$	0.102	0.264	0.372

From Table 2, it can be seen that for non-faulty operation the $\epsilon_{RMS,30}$ is 0.102, a value which complies with the ANN properties definition and ANN training values shown in Table 1. For faulty operation, the values of the $\epsilon_{RMS,30}$ are 0.264 for bias and 0.372 for precision degradation. Since the $\epsilon_{RMS,30}$ values for both sensor faults exceed the predefined threshold, it is concluded that both faults are efficiently and accurately diagnosed by the proposed fault diagnosis approach.

5. Summary and conclusions

To ensure the reliable and consistent performance of SHM systems, sensor faults must be accurately and efficiently detected. Common fault diagnosis approaches, in both cable-based and wireless SHM systems, use raw structural response data for fault diagnosis. However, in wireless SHM systems, the wireless communication of raw data entails considerable power consumption. In this paper, a fault diagnosis approach using processed structural response data and the concept of analytical redundancy has been presented. In the proposed approach, fault diagnosis is based on the correlations among Fourier amplitudes of structural response data derived from different sensors at a given structural condition. The Fourier amplitude at the peak corresponding to the fundamental eigenfrequency is predicted at each sensor node, using the Fourier amplitudes of other sensor nodes as input data and implementing artificial neural networks (ANNs) in an entirely data-driven approach. Deviations between the predicted Fourier amplitude and the actual Fourier amplitude calculated from newly collected acceleration response data are indicative of faulty sensor operation.

Validation tests of the fault diagnosis approach have been conducted on a 4-story laboratory frame structure. A fault-tolerant wireless SHM system prototype has been implemented to validate the proposed approach. The wireless SHM system has been installed on the laboratory frame structure. First, the ANN properties have been defined based on prediction accuracy and performance criteria. Then, two fault types, bias and precision degradation, have been considered for testing the wireless SHM system under faulty sensor operation. The results from the faulty sensor operation have shown that the residuals between the predicted Fourier amplitudes and the actual Fourier amplitudes are indicative of sensor faults. It is clear that the efficiency of the proposed fault diagnosis approach depends on the effect of the sensor fault on the amplitude at the selected peak of the frequency spectrum. Importantly, if

the eigenfrequency is altered, the embedded ANNs are able to retrain and adapt to the new structural condition. Future research will focus on the applicability limits of the proposed approach, as well as the suitability of the approach to diagnose other various fault types.

Acknowledgments

The authors would like to gratefully acknowledge the support offered by the German Research Foundation (DFG) under grant GRK 1462 (“Evaluation of Coupled Numerical and Experimental Partial Models in Structural Engineering”). The financial support is gratefully acknowledged. Any opinions, findings, conclusions or recommendations expressed in this paper are those of the authors and do not necessarily reflect the views of DFG.

References

- Basirat, A. H. and Khan, A. I. (2009). “Graph neuron and hierarchical graph neuron, novel approaches toward real time pattern recognition in wireless sensor networks”. In: Proc. of the 2009 International Conference on Wireless Communications and Mobile Computing. Leipzig, Germany, 21/06/2009.
- Brincker, R., Andersen, P. and Zhang, L. (2000). “Modal identification from ambient responses using frequency domain decomposition”. In: Proc. of the 18th International Modal Analysis Conference (IMAC), San Antonio, TX, USA, 07/02/2000.
- Cooley, J. W. and Tukey, J. W. (1965). “An algorithm for the machine calculation of complex Fourier series”. *Mathematics of Computation*, Vol. 19, No. 90, pp. 297-301.
- Dragos, K. and Smarsly, K. (2015). “A comparative review of wireless sensor nodes for structural health monitoring”. In: Proc. of the 7th International Conference on Structural Health Monitoring of Intelligent Infrastructure. Turin, Italy, 01/07/2015.
- Jahr, K., Schlich, R., Dragos, K. and Smarsly, K. (2015). “Decentralized autonomous fault detection in wireless structural health monitoring systems using structural response data”. In Proc. of the 20th International Conference on the Applications of Computer Science and Mathematics in Architecture and Civil Engineering (IKM). Weimar, Germany, 22/07/2015.
- Kraemer, P. and Fritzen, C.-P. (2007). “Sensor Fault Identification Using Autoregressive Models and the Mutual Information Concept”. *Key Engineering Materials*, Vol. 347, pp. 387-392.
- Kriesel, D. (2007). “A brief introduction to neural networks”. Available at: <http://www.dkriesel.com>.
- Obst, O. (2009). “Distributed fault detection using a recurrent neural network”. In: Proceedings of the 2009 International Conference on Information Processing in Sensor Networks. Washington, DC, USA, 13/04/2009.
- Oracle Corp. (2010). “Sun SPOT eDEMO Technical Datasheet, 8th edition”. Sun Labs, Santa Clara, CA, USA, 2010.
- Qin, S. J. and Li, W. (1999). “Detection, identification, and reconstruction of faulty sensors with maximized sensitivity”. *Journal of American Institute of Chemical Engineers*, Vol. 45, No. 9, pp. 1963-1976.
- Smarsly, K. and Petryna, Y. (2014). “A Decentralized Approach towards Autonomous Fault Detection in Wireless Structural Health Monitoring Systems”. In: Proc. of the 7th European Workshop on Structural Health Monitoring. Nantes, France, 08/07/2014.
- Smarsly, K. and Law, K. H. (2014). “Decentralized fault detection and isolation in wireless structural health monitoring systems using analytical redundancy”. *Advances in Engineering Software*, Vol. 73, pp. 1-10.
- Venkatasubramanian, V., Vaidyanathan, R. and Yamamoto, Y. (1990). “Process fault detection and diagnosis using neural networks – 1. Steady-state processes”. *Computers & Chemical Engineering*, Vol. 14, No. 7, pp. 699-712.
- Willsky, A. S. (1976). “A survey of design methods for failure detection systems”. *Automatica*, Vol. 12, pp. 601-611.